

Impairment-aware Virtual Network Embedding Using Time Domain Hybrid Modulation formats in Optical Networks

Original

Impairment-aware Virtual Network Embedding Using Time Domain Hybrid Modulation formats in Optical Networks / Shahzad, Farooq; Khan, Ihtesham; Masood, Muhammad Umar; Ahmad, Arsalan; Imran, Muhammad; Ruffini, Marco; Curri, Vittorio. - ELETTRONICO. - (2021), pp. 1-6. (Intervento presentato al convegno 2021 International Conference on Optical Network Design and Modeling (ONDM)) [10.23919/ONDM51796.2021.9492380].

Availability:

This version is available at: 11583/2915891 since: 2021-07-30T11:17:17Z

Publisher:

IEEE

Published

DOI:10.23919/ONDM51796.2021.9492380

Terms of use:

This article is made available under terms and conditions as specified in the corresponding bibliographic description in the repository

Publisher copyright

IEEE postprint/Author's Accepted Manuscript

©2021 IEEE. Personal use of this material is permitted. Permission from IEEE must be obtained for all other uses, in any current or future media, including reprinting/republishing this material for advertising or promotional purposes, creating new collecting works, for resale or lists, or reuse of any copyrighted component of this work in other works.

(Article begins on next page)

Impairment-aware Virtual Network Embedding Using Time Domain Hybrid Modulation formats in Optical Networks

Farooq Shahzad

National University of Sciences
& Technology (NUST), Pakistan
fshahzad.msee16seecs@seecs.edu.pk

Ihtesham Khan

DET, Politecnico di Torino, Italy
ihtesham.khan@polito.it

M Umar Masood

DET, Politecnico di Torino, Italy
muhammad.masood@polito.it

Arsalan Ahmad

National University of Sciences
& Technology (NUST), Pakistan
arsalan.ahmad@seecs.edu.pk

Muhammad Imran

Scuola Superiore Sant'Anna, Pisa, Italy
muhammad.imran@santannapisa.it

Marco Ruffini

Trinity College Dublin, Ireland
marco.ruffini@tcd.ie

Vittorio Curri

DET, Politecnico di Torino, Italy
curri@polito.it

Abstract—The rapid increase in bandwidth-intensive applications has resulted in the progressive growth of IP traffic volume, especially in the backbone networks. To address this growth of internet traffic, operators are searching for innovative solutions which avoid new installation and replacement of the existing network infrastructure. In this context, efficient spectrum utilization is one of the key enablers to extract the residual network capacity. This paper proposes an innovative algorithm exploiting electronic traffic grooming and using impairment-aware routing to address the virtual network embedding problem (IA-TG-VNE) in optical networks. We also analyze the networking benefits of using time-domain hybrid modulation formats (TDHMF) over four conventional modulation formats; binary phase-shift keying (BPSK), quadrature phase-shift keying (QPSK), 16 quadrature amplitude modulation (QAM), and 64 QAM. The analysis is performed on a detailed physical layer model based on the Gaussian Noise (GN) model, which includes the effect of both linear and nonlinear impairments. The simulation results are obtained on realistic network topology: a 37-nodes PAN-EU. The simulation results show that TDHMF always performs better than conventional modulation formats for all types of fiber in terms of total network capacity, the average bit rate per lightpath (LP), number of LPs, and request blocking ratio.

Index Terms—Virtual Network Embedding, Time domain hybrid modulation formats, Wavelength Division Multiplexing.

I. INTRODUCTION

The technological innovations continually introduce revolutionary applications and solutions, influencing the way people interact, make decisions, and conduct business. These applications/solutions require high speed, improved capacity and adaptability of high speed optical networks. As a result, an annual traffic growth of 6% is expected between 2018 and 2023 [1]. To cope with this increase in data traffic, operators are constantly looking for solutions to increase capacity and improve the adaptability of the existing network infrastructure. Ideally, this should be achieved by avoiding updating the installed fibers and optical devices in order to save high costs

for replacing installed equipment and reinstalling [2]. Flexible transceivers have been proposed to support reconfigurable capacity and range based on traffic and network conditions. This flexibility is achieved by reconfiguring one or more transceiver parameters such as modulation format, symbol rate (R_s) and forward error correction (FEC) [3], [4]. However, operators prefer to have flexibility with minimal additional cost. One such strategy is to install new flexible transponders while connecting them to fixed-grid, baud rate and multiplexing devices. Bit rate flexibility can be achieved by affecting the bit rate with the optical signal-to-noise ratio (OSNR). The modulation format can be adapted to the multitude of lower or upper constellations based on the available OSNR. However, the multitude of constellations usually follow the $2^M QAM$ granularity steps, which leads to discrete bit per symbol (BpS) (2, 4, 8, 12); therefore, giving discrete values of the bit rate ($R_b = R_s * BpS$). To have the flexibility of the fine granular bit rates, i.e., fractional BpS, hybrid time-domain modulation (TDHMF) formats have been proposed [5], [6]. Depending on the available/required LP-OSNR, the TDHMF can continuously adjust the BpS value, which increases the flexibility and efficiency of the network. TDHMF transmission is the time domain combination of two modulation formats that offer better bit rate coordination over a range with guaranteed transmission quality (QoT). TDHMF, however has a compromise between bit rate optimization and optical range. However, previous studies of point-to-point connections in a network show that TDHMF is an effective technique in terms of transmission capacity [7]. The introduction of TDHMF to improve the capacity/efficient use of the spectrum of optical networks has received considerable attention recently. Several publications have been reported in which the TDHMF approach has been assessed at the physical or network level, and in some cases at both levels. In [5], the authors evaluated the influence of non-linear fiber propagation on TDHMF and Flex-PAM

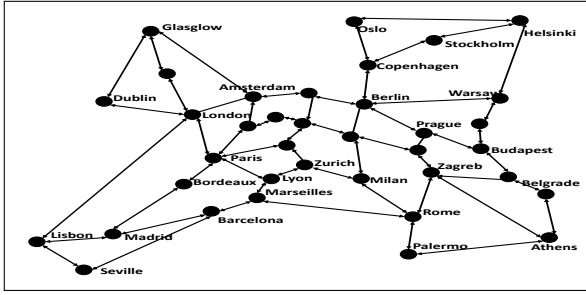


Fig. 1: PAN-EU Topology

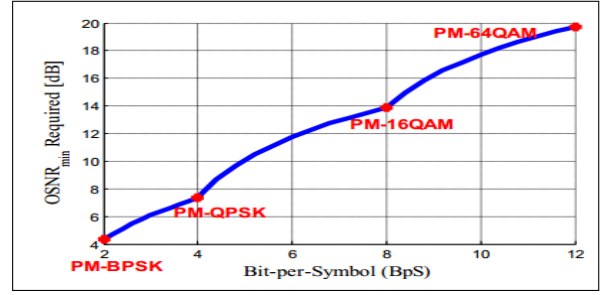


Fig. 2: $OSNR_{min}$ Required vs. BpS

using a flexible transponder. In addition, countermeasures are taken to interleave the polarization in order to reduce the TDHMF nonlinear propagation. The authors considered several transmission operating strategies for SSMF only, without any traffic grooming. In [6], the operating approaches of the transmitter were verified for the TDHMF technology, the minimal BER strategy produced the best results out of the four proposed strategies. In TDHMF, the nonlinear propagation penalty can be reduced by using pre-distortion and polarization interleaving. The TDHMF technique was only carried out for two fiber types: SSMF and NZDSF, without taking traffic grooming into account. In [8], a new DSP architecture has been proposed to identify and recognize any modulation format, including TDHMF signals consisting of BPSK/QPSK/16 QAM/64 QAM. The DSP architecture was used for software-defined coherent optical receivers that successfully identified the modulation format with no previously received signal information. In [9], in order to improve network capacity, a hybrid Raman amplifier (HFA) in a transparent fixed-grid optical network has been proposed. The well-known problem of routing and wavelength allocation with logical topology design (LTD-RWA) is solved by simply creating a direct LP (First-Fit) without carrying out any traffic grooming. The influence of HFA on PMF and TDHMF is examined for three typical fiber types: SSMF, NZDSF and PSCF. In contrast to the work is already done, this work proposes a traffic grooming and impairment-aware routing algorithm to embed virtual network (IA-TG-VNE) using TDHMF over a substrate physical WDM (Wavelength Division Multiplexing) network. This work highlights the advantage of traffic grooming and impairment-aware routing on a realistic network and multiple performing parameters. In order to obtain more meaningful and precise results, we first define suitable models for both the physical and the network layer of the optical network under consideration. In addition, we compare the results for three typical fiber types: standard single-mode fiber (SSMF), non-zero dispersion shift fiber (NZDSF), and pure silica core fiber (PSCF). The performance is analyzed based on the variable power per channel (P_{ch}) for the physical and average traffic per node on the network layer. TDHMF performance is assessed based on total network capacity, the average bit rate per LP, request blocking ratio, and the number of LPs. The simulation results in the PAN-EU network with 37 nodes and 114 bidirectional connections (see Fig. 1 [10]) show that

TDHMF always works better than modulation formats that are based only on discrete values of BpS.

II. TRANSMISSION LAYER MODEL

Choosing an accurate transmission model is critical to evaluating network performance. With this aim in mind, we consider the detailed model of the physical layer based on the GN model [11]. This includes both amplified spontaneous emission noise (ASE) caused by EDFA and non-linear interference (NLI) due to the non-linear propagation of fibers. The optical signal-to-noise ratio (OSNR) used as a performance parameter is expressed as;

$$OSNR_{i,j} = \frac{P_{ch}}{N_s[P_{ASE} + \eta P_{ch}^3]} \quad (1)$$

$$OSNR = \frac{1}{\sum_{i=1}^{N_{Nodes}-1} \frac{1}{OSNR_{i,i+1}}} \quad (2)$$

N_s is the number of spans, P_{ASE} , the spontaneous noise amplified by EDFA, P_{ch} the power per channel, η , the efficiency of NLI generation in each fiber span for the worst case light-path and $OSNR_{i,j}$ is OSNR on a link that connects two nodes i and j . The amplifiers are arranged on a span of $L_s = 100$ km and consist of homogeneous and uncompensated reinforced fiber links. Three different types of fibers that are considered for link analysis are SSMF, NZDSF, and PSCF. The optical properties of these fiber types such as attenuation coefficient (α), dispersion coefficient (D), non-linearity coefficient (γ) and effective area (A_{eff}) are shown in Tab. I. EDFA's ASE noise is considered to be approximated as:

$$P_{ASE} = hf_o(G-1)FR_{SG} \quad (3)$$

where h is the Plank's constant, f_o is the center frequency, the noise figure F is considered as 5 dB, the amplifier gain is known as G and R_{SG} is the symbol growth rate. We consider the maximum output power $P_{MAX} = +1$ dBm / channel. The total OSNR of the entire route is derived from Eq. 2, where N_{node} is the number of network nodes that the working LP traverses. We consider polarization multiplexed (PM) multilevel modulation formats, which are followed by a set of four square modulation formats: PM-BPSK, PM-QPSK, PM-16QAM, PM-64QAM and which are used as PMF. Fig. 2 shows $OSNR_{min}$ and BpS, which are required for both PMF and TDHMF [12]. The corresponding Bps values for these polarization multiplexed modulation formats are 2, 4, 8 and 12. The Bps values for TDHMF can have non-discrete values and can range from 2 to 12, since TDHMF continuously

uses two modulation formats. We consider modulation formats operating at gross symbol rate $R_{s,g} = 32Gbd$ per channel, resulting in a net symbol rate $R_s = 25Gbd$ per channel due to 25% coding and protocol overhead. We analyze the system when the all-optical C-band is available ($B_{opt} = 4THz$). Therefore, the number of channels is 80 on a single point-to-point fiber link with a channel spacing of 50 GHz.

TABLE I: Fiber Characteristics [13]

Fiber	α [dB/km]	D[ps/nm/km]	γ [1/W/km]	A_{eff} [μm^2]
PSCF	0.165	20.4	0.8	135
SMF	0.200	16.5	1.3	80
NZDSF	0.222	3.9	1.6	70

III. NETWORK LAYER MODEL

We consider an IP over a WDM network with fixed a spectrum distribution. In the physical network topology, physical links connect nodes to other nodes on an existing network. The physical topology of the network can be represented as graph $g(V, E)$, with the vertices (V) representing the nodes connected to the edges (E) which represent the physical fiber connections. We assume that the fibers between the nodes are provided in pairs of equal physical length, thereby providing bi-directional connectivity between the pairs of nodes. Each node in the network is equipped with an Optical Cross-Connect (OXC), a transponder and an IP router. OXC is responsible for transparent LP routing and switching. The physical connection between the nodes i and j is specified with $D_{i,j}$, measured in km; while $D_{i,j} = D_{j,i}$. We consider the traffic matrix to be a set of asymmetric IP traffic requirements expressed in Gb/s between all source and destination pairs. The traffic requests generated by the source nodes are transmitted over optical channels consisting of one or more physical links over one or more successive LPs to their final destinations. In this case, requests between successive LPs are processed electronically by the IP routers. The virtual network is the set of all previously established LPs that meet all traffic requirements. At the intermediate nodes, OXC changes the LP transparently. Flexible OFDM (Orthogonal Frequency Division Multiplexing) transponders are used to generate each LP in the source node and terminate at the destination node. The flexible OFDM transponder has a maximum transmission capacity C_{MAX} of 300 Gb/s; with the ability adapt to any modulation format to carry the traffic demand on an LP based upon the optical range from the source to the destination. The modulation format is selected according to the required OSNR. Depending on the modulation format, each LP has a certain transmission rate and a certain optical range.

Depending on the selected modulation format, the LP created for a short distance runs at a very high bit rate and the LP was created for a long-distance runs at a low bit rate. The network model first defines the set of LPs that meet all traffic requirements, i.e. virtual network embedding (VNE). Each LP is created with a particular modulation format based on the optical range and a particular wavelength is assigned using the first-fit, taking into account both the continuity of the wavelength and the contiguity constraints. Under these

conditions, the assigned wavelength of one LP never overlaps the assigned wavelengths of other LPs on the same physical link. Finally, the virtual network is formed, which carries out all traffic requests with constraints over the wavelengths assigned by an LP on the physical links.

IV. NETWORK DESIGNING UNDER A DETAILED TRANSMISSION LAYER MODEL

The electronic traffic grooming scheme was developed in [14] to increase network resource usage and channel efficiency. This work proposes an IA-TG-VNE algorithm to obtain the simulation results shown in Alg. 1. The proposed IA-TG-VNE algorithm is derived from [15], which performs electronic traffic grooming and determines the required LP based on the impairment-aware routing. The IA-TG-VNE algorithm contains a more detailed transmission layer model by performing the computation of the OSNR value in the destination node of each LP. This allows to define a more realistic planning, as the transmission range for different modulation formats is more realistic than the simpler model implemented in [15], which is based on the precalculated table for each modulation format could be used up to a certain distance. The IA-TG-VNE proposal first checks the maximum transmission range, consider length of the physical path according to Eq. 2 as described in Section III. The IA-TG-VNE based on the GN model [11], that encapsulates both linear and non-linear impairments. It is assumed that all connections are fully loaded to avoid a reconfiguration of already established LPs since according to the GN model [11], the OSNR decreases as the number of channels in the physical connection increases. A worst-case scenario is therefore assumed for the calculation of η_{NLI} . The required OSNR is compared with the obtained OSNR in order to determine the optical range against the OSNR trade-off for the selection of the appropriate modulation format. The proposed IA-TG-VNE algorithm solves the problem of virtual network embedding. The IA-TG-VNE algorithm creates the LP to meet the highest traffic requirements first. This algorithm limits the LP creation process by adjusting the upcoming traffic requests on existing LPs when enough capacity is available to support this traffic request. If the existing LPs cannot support the traffic requirement, a new LP is created to satisfy the traffic. In this case, the IA-TG-VNE algorithm creates a new LP with a specific modulation format according to the required OSNR. The algorithm continues this process until all traffic requirements are met. The resulted set of LPs are then forwarded to the underlying physical topology using a first-fit wavelength assignment approach considering the wavelength contiguity and continuity constraints. Suppose capacity is available on the existing LP. In that case, there is no extra cost to pay for traffic grooming in terms of extra power consumption because transponders with a capacity of 300 Gbps are already placed in the network. At intermediate nodes, the larger capacity router is mandatory to accommodate the extra traffic, creating an additional overhead of power consumption. However, this power consumption is negligible

Algorithm 1 Impairment Aware traffic Grooming Heuristic based on Virtual Network Embedding (IA-TG-VNE)

```

Require: :  $\mathcal{P}_{sd}, \forall (s, d) \in \tau, \zeta$ 
Ensure: :  $\Gamma$ 
1: for all  $\zeta_{sd} \in \zeta$  do
2:   if LP available and  $\zeta_{sd} \leq Capacity(l_{sd})$  then
3:      $allocate\_demand(\zeta_{sd}, l_{sd});$ 
4:   else
5:     if path available and  $\zeta_{sd} \leq Capacity(\mathcal{P}_{sd})$  then
6:        $allocate\_demand(\zeta_{sd}, \mathcal{P}_{sd});$ 
7:        $groomed - \Gamma = select - LP(\mathcal{P}_{sd}, \forall (s, d) \in LP);$ 
8:     else
9:       LP = compute-LP ( $\Gamma, s, d$ )
10:    end if
11:  end if
12:  if LP is void then
13:     $demand - satisfied \leftarrow \text{false};$ 
14:     $p = shortest - path(\mathcal{P}_{sd});$ 
15:     $\Gamma = dir - lightpath - allowed(\zeta_{sd}, \Gamma)$ 
16:    while dir-lightpath feasible (p) is true and demand-satisfied is false do
17:       $OSNR_{\phi} = compute - OSNR(\zeta_{sd}, \phi);$ 
18:       $m = select - modulation(\zeta_{sd}, p, OSNR_{NL}^p);$ 
19:       $\lambda_{sd} = compute - lambda - required(\zeta_{sd}, m);$ 
20:      if  $\lambda_{sd} - available(p)$  then
21:         $establish - lightpath(\zeta_{sd}, \phi, m);$ 
22:         $demand - satisfied \leftarrow \text{True};$ 
23:      else
24:         $p = next - shortest - path(\mathcal{P}_{sd});$ 
25:      end if
26:    end while
27:    if  $demand - satisfied$  is false then
28:      while path-exits(p) is true and demand-satisfied is false do
29:         $SP = break - path(p);$ 
30:         $subpaths - feasible = check - subpath(\zeta_{sd}, SP);$ 
31:        if subpath-feasible is true then
32:           $establish - subpaths - lightpaths(\zeta_{sd}, SP);$ 
33:           $demand - satisfied \leftarrow \text{True};$ 
34:        else
35:           $p = next - shortest - path(\mathcal{P}_{sd});$ 
36:        end if
37:      end while
38:    end if
39:    if demand-satisfied is false then
40:      return Block-request;
41:    end if
42:    if  $\Gamma$  is void then
43:      return Block-request;
44:    end if
45:  end if
46: end for
47:  $assign - \lambda_{sd} = assignment \lambda$  on respective wavelength considering constraints ( $\Gamma$ )
48: if assign- $\lambda$  is true then
49:   return  $\Gamma$ 
50: else
51:   return Block-request
52: end if

```

as compared to the excellent results of the IA-TG-VNE algorithm shown in the next section.

In addition, we calculated the OSNR in the destination node of each LP. The calculated OSNR is compared to the required OSNR (at the FEC limit) to find the modulation format suitable for the required optical reach.

A. Algorithm Description

The IA-TG-VNE pseudocode is represented in the Algo. 1 algorithm and works as follows:

- For each traffic request $\zeta_{s,d}$, the shortest path p between the source and the destination node is calculated and its QoT feasibility analyzed. A path p is considered QoT-feasible if its available $OSNR_{NL}^p$ is greater than the

minimum OSNR required for the modulation format with the lowest cardinality, i.e. in our case PM-BPSK.

- If the LP is QoT-feasible, the highest cardinality modulation format m can be supported in a single slot based on the available $OSNR_{NL}^p$. The wavelength of the corresponding number required to send the traffic request $\zeta_{s,d}$ is calculated using the selected modulation format. If this number is greater than the maximum capacity of a single transceiver, which is 300 Gbps in this work, the request will be split across two or more wavelengths.
- The availability of a continuous set of spectral slots is then checked over the fiber links that are part of the path p . If such a continuous set is found, the LP is created and the request is assigned to it.
- If the requirement $\zeta_{s,d}$ cannot be assigned on the shortest path, the same procedures as in steps 1 to 3 are repeated, taking into account the next shorter path, until the requirement is met or up to the point at which there are no more LPs that can be reached with feasible QoT.
- If a traffic request cannot be allocated via the feasible QoT path, optically transparent allocation solutions are considered. In particular, the LP transparency is broken by inserting OEO in the intermediate nodes in order to obtain a set of valid QoT sub-paths. The OEO positioning strategy is pretty simple. This involves repeatedly computing the OSNR path from the source to all intermediate nodes by traversing the path back from the destination. We put a regenerator on the node, after which proceeding further to the next physical hop that will reduce $OSNR_{NL}^p$ below the required minimum OSNR of the lowest modulation format (i.e. PM-BPSK). After placing the regenerator in this intermediate node, let's consider this node as a virtual source node and repeat the process to see if more regenerators are needed. For each sub-path, the same procedures described in steps 1 to 3 are carried out to provisionally assign the request transparently. If these steps fail, other paths are considered. If the request $\zeta_{s,d}$ cannot be allocated, it is considered blocked.

V. SIMULATION RESULTS

We calculate our results on realistic network topologies: 37 nodes PAN-EU network. A custom-built event-driven tool in C language is used to run simulations for all three fiber types. The performance of the IA-TG-VNE algorithm for both techniques is measured by changing i) P_{ch} in (mW) from 0.036 to 1.236 and ii) average traffic per node in (Gb/s) that defined as the average of the total amount of traffic generated by a node. We generate ten average traffic values per node in the range of 500 Gb/s to 5000 Gb/s with a range of 500 Gb/s.

A. Importance of detailed Transmission Layer Model

We use a simple heuristic approach to calculate the total capacity of the network according to the theoretical calculation. It's different from the existing IGH algorithm [15] and proposed IA-TG-VNE algorithm. The proposed IA-TG-VNE algorithm is used to calculate all results except capacity. To

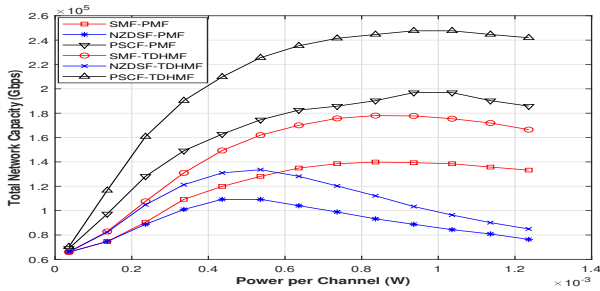


Fig. 3: Total Network Capacity vs. Power per Channel on PAN-EU Network

calculate the total network capacity, we consider an LP any-to-any matrix, i.e. establishing the LPs between all pairs of nodes of the PAN-EU network, obtaining a full network LP topology. Based on the optical reach, the bit rate of these LPs is calculated by assigning them an appropriate modulation format. The total network capacity using all three fiber types is calculated for both PMF and TDHMF by aggregating the bit rates of all LPs in the PAN-EU network. In this type of analysis, we examined how the variation of P_{ch} affects the performance of the network in order to compare the modulation techniques considered. With this in mind, we varied P_{ch} to get the total network capacity and request blocking ratio for both modulation strategies. The relationship between the total capacity of the network in relation to P_{ch} in the PAN-EU network is shown in Fig. 3. From the simulation results we can see that PSCF has greater network capacity than SSMF and NZDSF with both techniques: PMF and TDHMF. We also concluded that the TDHMF of all three fiber types had greater network capacity than the PMF of those fiber types, demonstrating the network advantages of TDHMF over PMF. In Fig. 3 all fibers have a larger network capacity with different values of P_{ch} , which is called the optimal value. PSCF, SSMF and NZDSF have an optimal value of P_{ch} 0.936 (mW), 0.736 (mW) and 0.436 (mW); respectively. In the absence of NLI, the ever-increasing trend could be observed for both (PMF and TDHMF), which is not correct. As explained in Section III, we considered the GN model. Due to the presence of NLI at the low and high values of P_{ch} , the network capacity has decreased, but the peak of the capacity is observed at the optimal values for each fiber type as shown in Fig. 3. The request blocking ratio is calculated using the proposed IA-TG-VNE algorithm taking into account the worst-case scenario with much higher traffic per node, i.e. 5000 Gb/s. In Fig. 4 without taking the NLI into account, we would observe the ever-decreasing trend, which is not true. Therefore, taking into account the NLI in Fig. 4 observes that the minimum request blocking ratio occurs at optimal values for each fiber. Similarly, increasing/decreasing P_{ch} causes the request blocking ratio to increase. Fig. 4 explains the relationship of the request blocking ratio with respect to P_{ch} for all three fiber types in the PAN-EU network. Referring to the Fig. 3 an opposite trend is observed in Fig. 4; the NZDSF request blocking ratio is higher because more requests

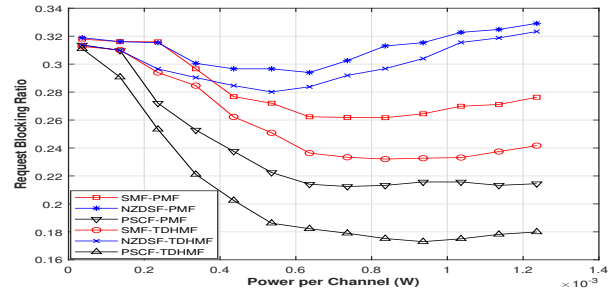


Fig. 4: Request Blocking Ratio vs. Power per Channel on PAN-EU Network

are blocked than the other two fiber types SSMF and PSCF. PSCF has the lowest request blocking ratio compared to SSMF and NZDSF. Therefore, TDHMF of all fiber types is best performed by blocking fewer requests than their respective PMF. The optimal value does not depend on the method of selection of the modulation format, but on the type of fiber used. Therefore, the remaining paper results were calculated with their optimal performance values per channel.

B. Capacity Analysis

Fig. 5 show the average bit rate for LP results obtained for the PAN-EU network. Each fiber type has two bars: solid for PMF and stripped for TDHMF. From Fig. 5 it can be seen that the TDHMF exceeds the PMF regardless of the fiber type and network topology as well as the performance of the TDHMF which depends on the size of the topology and the type of fiber. The percentage improvement of TDHMF compared to conventional modulation formats for each fiber type in both networks is shown in Fig. 5. From these results, we conclude that TDHMF works best in a large network and TDHMF can also improve the capacity of a fiber type with lower transmission quality. Concerning Fig. 5 TDHMF performed 40% better for NZDSF in the large PAN-EU network with 37 nodes than for NZDSF in the small 12-node Abilene network with 24%. TDHMF performance benefits are limited when TDHMF is delivered over a small network with a good quality fiber type. From Fig. 5 it can be seen that the hierarchy of the fiber types remains the same for both topologies, regardless of the type of topology. On a performance scale, PSCF leads SSMF and NZDSF. TDHMF and PMF show a higher average bit rate per LP on the same fiber types in the PAN-EU network compared to the Abilene network. Based on NZDSF as a reference, the advantages of PSCF for TDHMF always 62% regardless of the network topology. The benefits of all fiber types are much greater in the PAN-EU network, as the PAN-EU network is three times the size of the Abilene network. PSCF for PMF did 97% better than NZDSF, while PMF on the Abilene network did 73% better than NZDSF. For SSMF, the margin performance is around 33% for both; PMF and TDHMF in the Abilene network in relation to NZDSF, but in the PAN-EU network 46% and 57% in relation to PMF and TDHMF; respectively. From the previous results, we conclude that of all three typical fiber types, PSCF always offers the best performance and NZDSF has the lowest transmission quality.

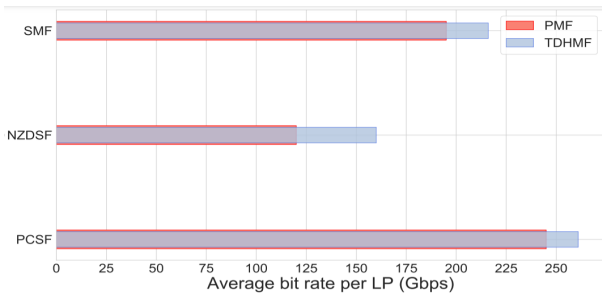


Fig. 5: Average Bit rate per LP PAN-EU Network

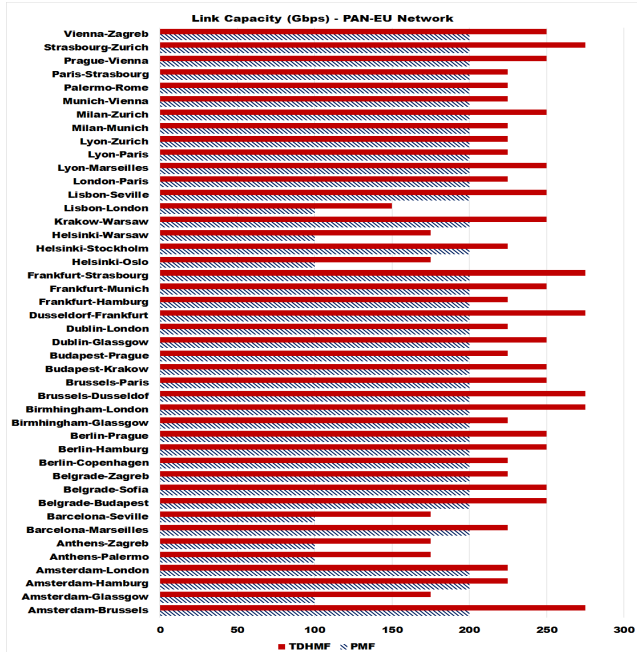


Fig. 6: Total Link Capacity on SSMF PAN-EU Network

The rest of the results are based on the SSMF fiber type. Hence we obtained results for all types of fibers. The fiber type hierarchy defined at network level for both topologies, however, remains the same for transmission from node to node. Due to a similar trend in fiber types and to maintain paper brevity, results are presented in only one fiber type, SSMF. The capacity of each fiber link is shown in Fig. 6 for the PAN-EU network. In the PAN-EU network, the TDHMF delivers the same results as the PMF for 13 links. The PAN-EU network consists of 37 nodes connected by 114 bidirectional links. Representing all of these relationships is difficult because the figure becomes so complex, so we're removing 13 links that offer the same performance. For 17 links, TDHMF outperforms PMF by 12.5%. For 14 links, TDHMF performs 25% better than PMF. TDHMF leads with 37.5% PMF for six links. For the only link between Lisbon and London, the TDHMF scores 50% better than the PMF. For six connections, TDHMF performs 75% better than PMF.

VI. CONCLUSIONS

We compared the transmission techniques of TDHMF with PMF in the PAN-EU network, taking into account a detailed

model of the physical layer. We have considered both linear and non-linear impairments in the physical layer model based on the GN model. We performed the simulation with an electronic traffic control algorithm based on impairment aware (IA-TG-VNE) for all three fiber types: SSMF, NZDSF and PSCF. By varying the power per channel (W) on the physical layer and the average traffic per node (Gb/s) on the network layer, TDHMF increases the overall capacity of the network. 20% for SSMF, 40% for NZDSF and 15% for PSCF compared to PMF. In addition, the results confirm that TDHMF outperforms PMF in terms of the number of LPs, with a 10% improvement for all three fiber types. For blocked requests, TDHMF exceeds PMF; this was 43% for PSCF; 31% for SSMF and 12% for NZDSF. Moreover, using the proposed IA-TG-VNE algorithm, TDHMF yielded the best of all combinations of modulation techniques.

Acknowledgement: This publication has been produced with co-funding of the European Union for the Asi@Connect Project under Grant contract ACA 2016-376-562.

REFERENCES

- [1] Cisco, "Cisco annual internet report," Cisco white paper p. 35 (2020).
- [2] G. Wellbrock and T. J. Xia, "How will optical transport deal with future network traffic growth?" in *ECOC, 2014*, (IEEE, 2014), pp. 1–3.
- [3] A. Napoli, M. Bohn, D. Rafique, A. Stavdas, N. Sambo, L. Poti, M. Noelle, J. K. Fischer, E. Riccardi, A. Pagano *et al.*, "Next generation elastic optical networks: The vision of the european research project idealist," *IEEE communications magazine* **53**, 152–162 (2015).
- [4] N. Sambo, D. Antonio, C. Porzi, V. Vercesi, M. Imran, F. Cugini, A. Bogoni, L. Poti, P. Castoldi *et al.*, "Sliceable transponder architecture including multiwavelength source," *JOCN* **6**, 590–600 (2014).
- [5] F. P. Guiomar, R. Li, C. R. Fludger, A. Carena, and V. Curri, "Hybrid modulation formats enabling elastic fixed-grid optical networks," *JOCN* **8**, A92–A100 (2016).
- [6] V. Curri, A. Carena, P. Poggiolini, R. Cigliutti, F. Forghieri, C. Fludger, and T. Kupfer, "Time-division hybrid modulation formats: Tx operation strategies and countermeasures to nonlinear propagation," in *OFC, 2014*, (IEEE, 2014), pp. 1–3.
- [7] H. Dai, Y. Li, and G. Shen, "Explore maximal potential capacity of wdm optical networks using time domain hybrid modulation technique," *JLT* **33**, 3815–3826 (2015).
- [8] P. Isautier, J. Langston, J. Pan, and S. Ralph, "Agnostic software-defined coherent optical receiver performing time-domain hybrid modulation format recognition," in *OFC, (OSA, 2015)*, pp. Th2A–21.
- [9] A. Ahmad, A. Bianco, H. Chouman, D. DeTommaso, G. Marchetto, S. Tahir, and V. Curri, "Merit of hybrid edfa/raman amplification in fixed-grid all-optical network exploiting multirate transponders," *IJCS* **31**, e3383 (2018).
- [10] I. Khan, A. Ahmad, M. U. Masood, A. W. Malik, N. Ahmed, and V. Curri, "Impact of data center placement on the power consumption of flexible-grid optical networks," *Optical Engineering* **59**, 016115 (2020).
- [11] P. Poggiolini, G. Bosco, A. Carena, V. Curri, Y. Jiang, and F. Forghieri, "The gn-model of fiber non-linear propagation and its applications," *JLT* **32**, 694–721 (2014).
- [12] A. Ahmad, A. Bianco, H. Chouman, D. DeTommaso, G. Marchetto, S. Tahir, and V. Curri, "Impact of fiber types and raman pumping in reconfigurable dwdm transparent optical networks," in *ECOC, 2015*, (IEEE, 2015), pp. 1–3.
- [13] A. Ahmad, A. Bianco, H. Chouman, G. Marchetto, S. Tahir, and V. Curri, "Impact of fiber type and raman pumping in nywdm flexible-grid elastic optical networks," in *ICTON, 2016*, (IEEE, 2016), pp. 1–4.
- [14] S. Zhang, C. Martel, and B. Mukherjee, "Dynamic traffic grooming in elastic optical networks," *J-SAC* **31**, 4–12 (2013).
- [15] A. Ahmad, A. Bianco, and E. Bonetto, "Traffic grooming and energy-efficiency in flexible-grid networks," in *ICC, 2014*, pp. 3264–3269.